Why Is There a Tritium Maximum in the Central Equatorial Pacific Thermocline?

ZHENGYU LIU AND BOYIN HUANG

Department of Atmospheric and Oceanic Sciences, University of Wisconsin—Madison, Madison, Wisconsin

ABSTRACT

It is suggested that the tritium maximum in the central Pacific is caused by two water pathways across the North Equatorial Countercurrent (NECC), one from the central Pacific and the other from the Mindanao Current. It is argued that an interior pathway exists, by which tritium-rich thermocline waters from the subtropical North Pacific cross the NECC in the central Pacific. The transport in this pathway, however, is small compared with that from the Mindanao Current.

1. Introduction

The spreading of tritium into the central equatorial Pacific thermocline (Fine et al. 1987) has provided evidence for the penetration of North Pacific water to the equator. Its most distinctive feature is an isolated maximum near the equator at about 140°W (Fig. 1a), which has been interpreted as a direct evidence of an equatorward ''interior water pathway'' that crosses the North Equatorial Countercurrent (NECC) in the central Pacific (Fine et al. 1987; McPhaden and Fine 1988). The strongest support for this interior water pathway comes, perhaps, from the tritium distribution itself on thermocline isopycnals. As shown in Figs. 1b,c (from Fine et al. 1981), these patterns show a ''blob'' of high values (indicated by the arrow) extending southeastward from north of 10°N at 160°W to south of 5°N at about 140°W. In the absence of an interior pathway, this ''blob'' seems very unlikely to exist.

McPhaden and Fine (1988, hereafter MF) first attempted a dynamical explanation for the central Pacific tritium maximum. They noticed that between 3°N and 14°N in the North Pacific, although the wind stress curl becomes positive (Fig. 2a), the Ekman pumping velocity field remains largely negative in the central Pacific (Fig. 2b). This negative Ekman pumping therefore allows a southward total geostrophic flow $V_G = f w_E / \beta$ across the NECC in the central Pacific, providing an essential piece of the interior pathway.

The argument of MF is incomplete. It does not con-

sider the vertical structure of the geostrophic flow and therefore cannot identify the source water of the geostrophic flow. Indeed, later in an intermediate model study, all the interior equatorward transport is found to occur entirely within the surface layer (Lu and Mc-Creary 1995, hereafter LM). This implies that all the interior pathway waters subduct in the Tropics, say, within about 20°N (shallow thermocline waters).

In observations, however, the tritium penetration occurs mainly in the deeper thermocline (Fine et al. 1981, 1987). For example, in Fig. 1a, the maximum tritium concentration occurs in the EUC core water of about $24 < \sigma_\theta < 26$. This tritium distribution implies that an equatorward penetration in the central Pacific, if it exists, should occur in the thermocline water that originates north of 20°N. This follows because, first, the $\sigma_\theta = 24$ isopycnal outcrops north of 20°N, even during later winter (Levitus 1982). Second, the maximum surface tritium concentration lies north of 20°N (Fine et al. 1981).

The main objective of this paper is to extend the work of MF to include the vertical structure of geostrophic flows. It is suggested that an interior pathway can exist that extends from the North Pacific toward the equator. The transport in this pathway, however, is small.

Our study also attempts to address the role of the Mindanao Current pathway in the central Pacific tritium maximum. McPhaden and Fine suggested that North Pacific water may also flow in a route through the Mindanao Current. Their study did not address the relative importance of the interior pathway and the Mindanao Current pathway, because they only used the Sverdrup theory, which does not apply to the boundary current. Our study suggests that the Mindanao Current pathway may be the dominant pathway. The dynamics of this pathway, however, seems to be complex.

Corresponding author address: Dr. Zhengyu Liu, Department of Atmospheric and Oceanic Sciences, University of Wisconsin—Madison, 1225 W. Dayton St., Madison, WI 53706-1695.
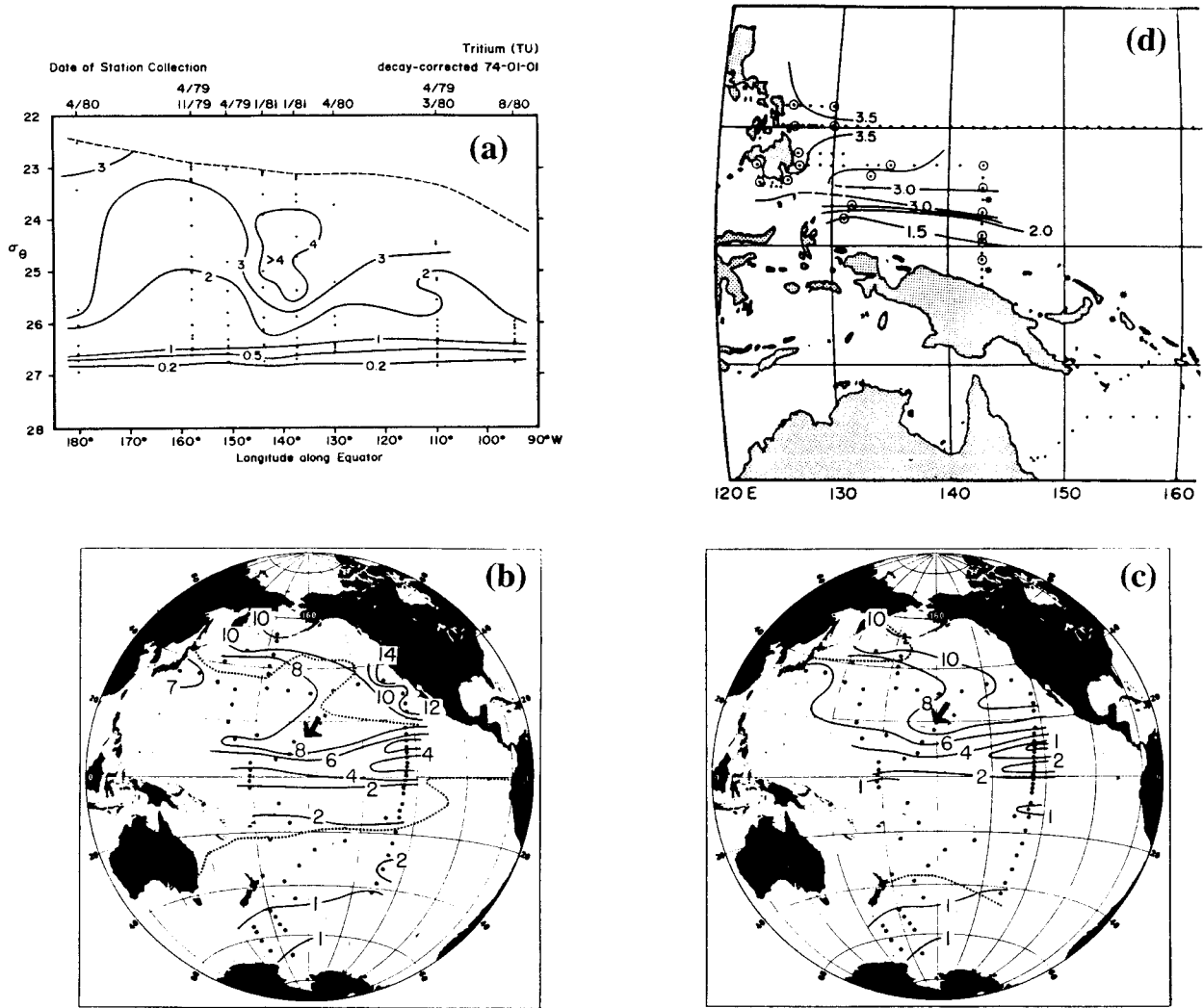E-mail: znl@ocean.meteor.wisc.edu

FIG. 1. Tritium distributions in the North Pacific. (a) Zonal equatorial section of tritium (TU) vs σ_θ. Tritium data decay corrected to 1 January 1974 (after Fine et al. 1987). (b) Tritium (TU) on the $\sigma_\theta = 23.9$ isopycnal. (c) Tritium (TU) on the $\sigma_\theta = 26.02$ isopycnal. In both (b) and (c), tritium concentrations have been adjusted for decay 1 January 1972 (after Fine et al. 1981). The arrows in both (b) and (c) indicate the "blob" of tritium penetration toward the equator. In the absence of an interior pathway, this blob seems very unlikely to exist. (d) Tritium (TU81N) in the layer 25.4–25.6 σ_θ (CI = 0.5 TU81N) (after Fine et al. 1994).

2. Equatorward penetration across NECC in the interior ocean

a. Basic mechanism

We start by reexamining the basic mechanism of the interior pathway. For simplicity, a simple ventilated thermocline model of Liu (1994) will be used (for more details, see Liu 1994). It has been pointed out that one sufficient condition for an interior pathway is for the ventilated zone to extend directly into the equatorial region before reaching the western boundary x_W (Liu 1994; McCreary and Lu 1994):

$$x_V(f) > x_w, \quad (1)$$

where $x_V(f)$ is the boundary of the ventilated zone and f is the Coriolis parameter. In a standard 2.5-layer ther-

mocline model, the first and second layers represent the upper and lower thermocline waters respectively. The former subducts from the Tropics (south of the outcrop line f_o), while the latter subducts from the subtropics (north of f_o). We will first consider the case of a zonally independent Ekman pumping $w_E(f)$. The boundary of the ventilated zone boundary can be derived as

$$x_V(f) - x_w = \frac{\beta\gamma_1}{2f^2 w_E(f)}\left[\left(1 - \frac{f}{f_o}\right)H_2\right]^2 + L, \quad (2)$$

where L is the width of the basin, and $\gamma_1 = g(\rho_2 - \rho_1)/\rho_o$ is the reduced gravity. The thickness of layer 2 and layer 1 along the eastern boundary are $H_2 =$ const and zero respectively. With the aid of (2), condition (1) can be written as a constraint for H_2:
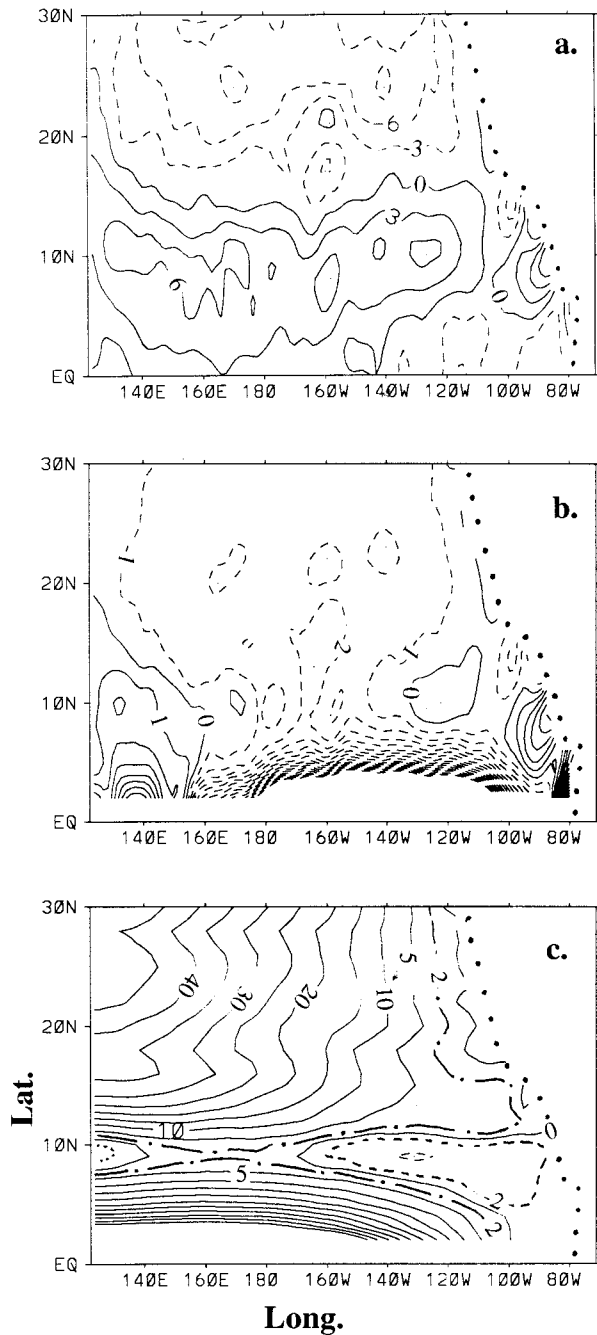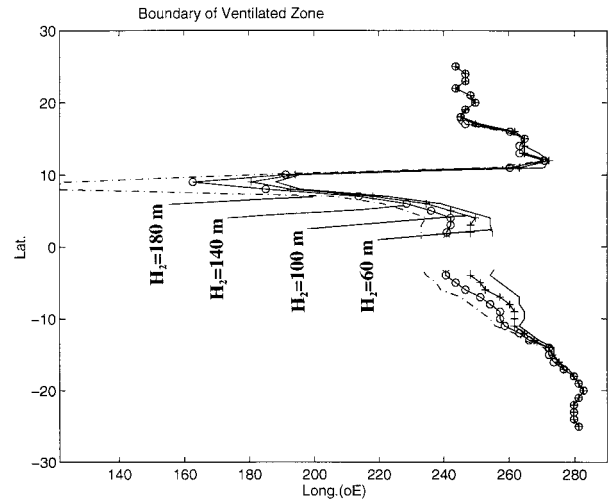
FIG. 3. The boundaries of the ventilated zone for outcrop line along 25°N in the Pacific under realistic annual mean wind forcing using the thermocline model in the appendix with four eastern boundary thickness of layer 2: H_2 = 180 m, 140 m, 100 m, and 60 m. The thickness of the first layer along the eastern boundary is set at zero. The mixed layer depth is set to zero. The reduced gravity are: $\gamma_1 = \gamma_2 = 1$ cm s^{-2}. (See appendix for more details.)

FIG. 2. (a) Wind curl (CI = 3 × 10^{-9} dyn cm^{-3}), (b) Ekman pumping (CI = 10^{-4} cm s^{-1}), and (c) total meridional geostrophic transport $(f/\beta) \int_{x_E}^{x} w_E(x, y)\, dx \,(= \int_{x_E}^{x} V_G\, dx)$ as in Eq. (1) (CI = 1) calculated from the annual mean FSU wind data. Dashed lines are for negative values.

$$H_2 < H_C \equiv \frac{f\sqrt{-2w_e(f)L/\beta\gamma_1}}{1 - f/f_0} \qquad (3)$$

for all f in the range of $f_D < f < f_0$, where f_D corresponds to the latitude where the planetary geostrophy assumption for the ventilated thermocline model fails

(the latitude of the order of the equatorial deformation radius, say, 5°N). A similar equation can also be obtained by rewriting the analytical solution of McCreary and Lu (1994), whose model combines the Ekman layer and the upper geostrophic layer of Liu (1994) into one layer.

According to (3), as long as the Ekman pumping is negative, the critical depth H_C remains positive and finite. Hence, the second-layer water can penetrate to the equator in the interior ocean if the second-layer thickness along the eastern boundary is shallower than the critical depth $H_2 < H_C$. Indeed, for a given Ekman pumping, the ventilated zone expands in layer 2 if layer 2 thickness is reduced (see discussion later on Fig. 3). This occurs because the change of potential vorticity that induces currents is determined by the change of the relative layer thickness, rather than the absolute layer thickness. Alternatively, from the continuity equation and geostrophic relationship, we have

$$O(\beta v_2) \sim O(\partial_x u_2 + \partial_y v_2) \sim O(\partial_z w_2) \sim O(w/h_2),$$

where the vertical velocity at the top of layer 2 is assumed to be the same order as the Ekman pumping. It is clear now that a thinner h_2 produces a stronger divergence field and, in turn, a stronger planetary geostrophic flow.

Under the condition that the zonal variation of Ekman pumping is not strong, (3) therefore states that the interior pathway from the subtropics exists as long as the Ekman pumping is negative at the latitude of the NECC. This has been further confirmed in a set of ocean general circulation model experiments with idealized settings (Huang 1996).

b. Application to North Pacific subtropical water

The 2.5-layer thermocline model can also be applied to the realistic Pacific. Figure 3 shows some examples of the ventilated zone boundaries for different H_2 (see the appendix for details of the calculation). The flow in the South Pacific is simple, because the Ekman pumping is negative throughout most of the tropical–subtropical region (not shown). As H_2 decreases, x_V expands eastward. Even for an H_2 as thick as 180 m, x_V still approaches the equator before it reaches the western boundary, indicating the existence of an interior water pathway.

In contrast, the North Pacific is much more complicated. This is mainly caused by the sign reversal of the Ekman pumping along latitudes of the NECC (Fig. 2b). It is seen in Fig. 3 that x_V extends toward the equator through the interior as long as H_2 is shallower than 140 m. [These ventilated zone boundaries resemble that of Talley (1985) in a 3.5-layer ventilated thermocline model.] However, the interior exchange is completely blocked if H_2 reaches 180 m because the curve of H_2 = 180 m hits the western boundary before reaching the equator. This case of a blocked ventilated zone boundary resembles that of LM.

The simple study above suggests an interior pathway that originates from the subtropical North Pacific. Crudely speaking, the interior pathway is possible on isopycnals that have their eastern boundary depths shallower than about 150 m. From Levitus (1982) data (not shown), this depth corresponds roughly to the depth of $\sigma_\theta = 26$ in the subtropics, which is close to the bottom of the thermocline. Therefore, it is possible for the main thermocline water that subducts in the subtropical North Pacific to cross the NECC in the central Pacific. This is consistent with the tritium observations in Figs. 1a–c, as well as some other observational studies. Mc-Phaden (1996) has found a southward geostrophic velocity at the depths of 100 to 300 m (about $10°C < T < 20°C$) at 7°N, 140°W. The maximum southward velocity reaches about 2 cm s^{-1} at the depth of about 200 m or about 15°C isothermal depth, which lies in the core of EUC. In addition, Wijffles (1993) has calculated the geostrophic transport across 10°N and found an interior transport of more than 3 Sv (Sv $\equiv 10^6$ m^3 s^{-1}) in the main thermocline. The latter two observations are Eularian observations; they are consistent with the presence of an interior pathway discussed above, although they cannot be regarded as direct confirmation of the Lagrangian interior pathway.

The simple model study also offers an explanation why the interior pathway is blocked in the layered model of LM: the thermocline layer thickness is set too thick. As shown in the sensitivity study in Table A1 (appendix), for reasonable parameters in the Pacific, the second layer thickness along the eastern boundary should not be thicker than 100–200 m (depending on other model parameters) for the existence of the interior pathway. In
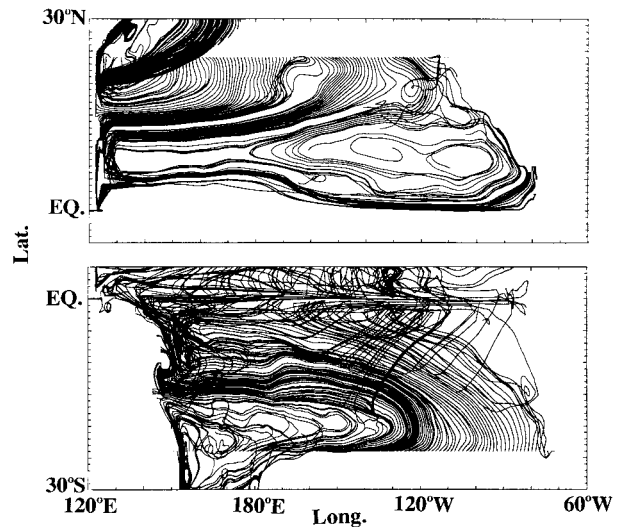

FIG. 4. Particle trajectories 19 years after subduction. The particles are initiated along 24°N and 24°S at the depth of 50 m. The velocity field is taken from the annual mean flow of the NCEP assimilated ocean data (Ji et al. 1995).

LM, however, the layer-2 depth along the eastern boundary is about 220 m. Our speculation is confirmed by a recent study of Lu et al. (1998) in their 3.5-layer intermediate upper-ocean model. After including diapycnal mixing, their model adjusts internally such that layer-2 thickness along the eastern boundary becomes shallower. They found that the interior pathway emerges if H_2 is shallow than about 180 m for their standard model parameters.

c. An OGCM study

As a further study, a Lagrangian analysis is carried out in a more realistic three-dimensional Pacific Ocean circulation, which derives its current field from the annual mean assimilated ocean data of the National Centers for Environmental Prediction (NCEP, Ji et al. 1995). Figure 4 shows the particle trajectories that subduct at 24°N (and 24°S). Various types of water pathways can be identified, as in Liu et al. (1994) and McCreary and Lu (1994). Here, we only need to notice the existence of the interior water pathway trajectories that originate from east of 140°W along 24°N and then cross the NECC in the central ocean between 160°W and 180°.

The total meridional geostrophic transport can be calculated from the surface Ekman pumping velocity as in Fig. 2c. Across the latitude of the NECC, the interior water transport is less than 7 Sv. This sets an upper bound for the transport of the interior pathway in the latitude range from 7° to 10°N (Liu 1994; McCreary and Lu 1994). A further analysis of the NCEP data (Huang 1996) shows a southward transport of about 2 Sv between 160°E and 140°W in the main thermocline (about $24 < \sigma_\theta < 26$). This transport is much smaller than the 10-Sv transport in the Mindanao Current. It is
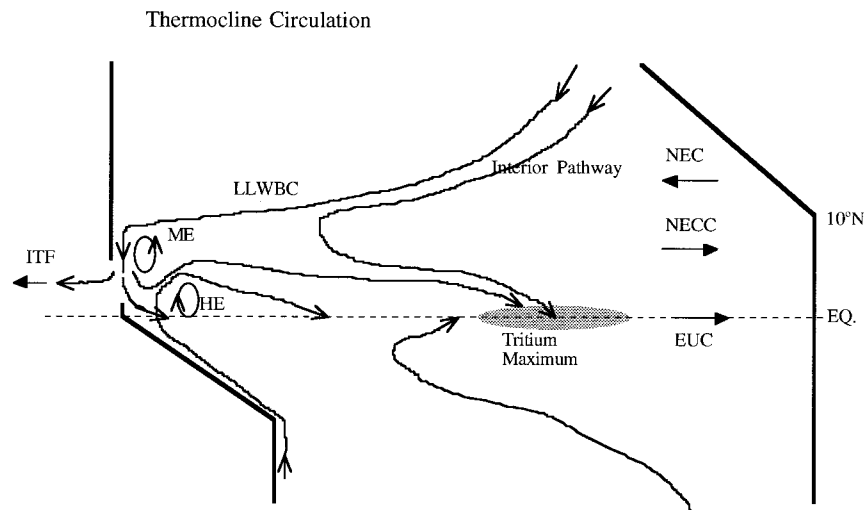
Thermocline Circulation

FIG. 5. Schematic figure of upper and middle thermocline circulation in the tropical–subtropical Pacific Ocean. The tritium maximum in the central equatorial Pacific is created by two sources of water from the North Pacific: one from the interior pathway and the other from the Mindanao Current. Notation is ME: Mindanao eddy, HE: Halmahera eddy, and ITF: Indonesian Throughflow.

therefore concluded that the equatorward penetration occurs through mainly the Mindanao Current, rather than the central Pacific. This conclusion is consistent with the recent study of Lu et al. (1998), who showed an interior transport of up to 3 Sv in a set of experiments.

3. Why is there a tritium maximum in the Central Equatorial Pacific?

Our study above raises a further question: If the water crosses the NECC predominantly through the Mindanao Current, why is the tritium maximum observed in the central equatorial region, rather than in the western equatorial region? This seems to be related to the complex nature of the Mindanao Current pathway.

Part of the clue may be found in the NCEP trajectory (Fig. 4). In contrast to the relatively simpler trajectories from the Southern Hemisphere, the trajectories in the Northern Hemisphere cross the NECC in a much more complex way. In particular, part of the Mindanao Current (from $10°$ to $5°$N) waters, after exiting the Mindanao Current, head back eastward into the interior ocean to join the NECC. These waters eventually join the EUC in the central Pacific, merging with the waters that cross the NECC in the interior ocean. Therefore, part of the Mindanao Current water forms a flow path of Mindanao–NECC–central Pacific. This seems to be consistent with the geostrophic transport near the equator calculated from hydrographic data (e.g., the 180 contour in Fig. 2a of Fine et al. 1987). It is also consistent with the total geostrophic flow calculated from the Ekman pumping forcing as in Fig. 2c, in which a substantial flow first exits the LLWBC and later join the NECC. (Of course, now one has to crudely treat the total geostrophic flow in Fig. 2c as a transport streamfunction.)

Therefore, the tritium maximum in the central equatorial Pacific can be caused by two sources of waters: one from the interior pathway and the other from the Mindanao Current. This is shown schematically in Fig. 5. Qualitatively, this flow picture is consistent with MF.

The nature of the peculiar pathway of Mindanao–NECC–central Pacific remains to be studied. Nevertheless, several mechanisms can be speculated here. First, the local Ekman pumping is positive in the region of Mindanao Current (west of $140°$E and south of $15°$N) as seen in Fig. 2b. This means that the interior geostrophic flow in this region is northward (also see Fig. 3 of MF). Therefore, after a southward water parcel passes $5°$N to exit the Mindanao Current, it tends to flow northeastward to join the NECC, rather than southeastward to join the EUC. Second, the strong Mindanao eddy also helps part of the Mindanao Current water to return northeastward (Fine et al. 1994; Tsychiya et al. 1989; Godfrey et al. 1993, 1996; Lukas et al. 1996). These two mechanisms may be related. Indeed, in a numerical model study, Masumoto and Yamagata (1991) have suggested that the Mindanao eddy is formed by the positive wind curl associated with the winter Asian monsoon. Third, there is evidence in both observations and numerical models that the waters from the Southern Hemisphere (New Guinea Coastal Undercurrent) overshoot across the equator and then retroflect eastward near the western boundary. This flow path may be related to the Halmahera eddy that is located about $2°$N (Tsychiya et al. 1989; Godfrey et al. 1993; 1996; Lukas et al. 1996). This cross-equatorial flow may still be able to prohibit a significant part of the Mindanao Current water from reaching the equator near the western boundary. This is consistent with the conclusion of Tsychiya et al. (1989) that most of the source water of the EUC

near the western boundary originates from the South Pacific. Indeed, the tritium distribution has a strong front near the western boundary at about 2°N (Fig. 1d from Fine et al. 1994). Similar frontal structures have also been observed in other tracers such as salinity and silica (Tsychiya et al. 1989).

4. Summary and discussions

We have addressed two questions related to the tritium maximum in the central equatorial Pacific. First, is there an interior pathway in the North Pacific? We have extended the works of MF and LM and found their discrepancy can be largely resolved. An interior pathway is likely to exist in the North Pacific main thermocline, but its transport is much smaller than that from the Mindanao Current.

Second, is the stronger Mindanao Current pathway consistent with the observed tritium maximum in the central equatorial Pacific? Based on model results and observations, we speculate that a significant part of the Mindanao Current water joins the EUC, not near the western boundary but, in the central Pacific. These waters first join the NECC after exiting the Mindanao Current and eventually penetrate equatorward in the central Pacific. Therefore, the tritium maximum in the central equatorial Pacific is caused by both waters in the interior and in the Mindanao Current.

Finally, some important questions regarding the water pathway still remain to be understood. One standing problem is the distribution of salinity in the central Pacific thermocline. The salinity there shows a front at about 10°N that seems to block the salinity tongue from the North Pacific (e.g., Fig. 2c of Wyrtki and Kilonsky 1984). In addition, the salinity near the equator also seems to be dominanted by the high salinity tongue from the Southern Hemisphere. This is in contrast to tritium, which shows a penetration from the North Pacific to the equator in the central Pacific (Figs. 4 and 5 of Fine et al. 1987). This strong north–south asymmetry of salinity could be caused by the complex surface salinity distribution (N. Nasami 1996, personal communication). For example, the heavy precipitation in the ITCZ can significantly dilute the salinity from the North Pacific, creating the salinity front near 10°N. Notice that the central Pacific EUC, and in turn the salinity, is contributed to by the waters from not only the interior pathway, but also the western boundary pathway; one can only infer from the asymmetric salinity field in the EUC that the EUC receives water more from the South Pacific than from the North Pacific.[1] It is yet unclear if this salinity field can be interpreted as direct evidence of the lack of an interior pathway from the North Pacific.

---

[1] This is consistent with our estimate from the NCEP data, which shows respectively about 10 Sv in the interior and the LLWBC pathways from the South Pacific (Huang 1996).

APPENDIX

The Boundary of the Ventilated Zone

In a coupled mixed layer/2.5-layer thermocline model, the boundary of the ventilated zone $x_v(f)$ is determined by (Liu 1994)

$$\frac{\gamma_2}{\gamma_1} D[x_V(f), f] = \left[\left(1 - \frac{f}{f_0}\right)H + \frac{f}{f_0}H_{s0}\right]^2 - H_s^2(f),$$
(A1)

where H = const and H_s are the total and mixed layer thickness along the eastern boundary $x = X_E f$, $D(x, f) = 2f^2 \int_{X_E}^x w_e(x, f)\, dx/\beta\gamma_2$, $\gamma_1 = (\rho_2 - \rho_1)/\rho_o$, and $\gamma_2 = (\rho_3 - \rho_2)/\rho_o$. The mixed layer density has been prescribed to vary linearly with latitude and the thickness of layer 1 is assumed to be zero along the eastern boundary. The mixed layer depth is assumed zonally uniform and its depth at the outcrop line f_0 is denoted by H_{s0} (see Liu 1994 for more details).

For a general Ekman pumping forcing and eastern boundary coastline, the boundary for the ventilated zone at a latitude of f can be found by integrating (A1) from the eastern boundary westward until the left-hand side equals the right-hand side. Table A1 shows the values of maximum H_2 that allows for an interior pathway in the North Pacific under different reduced gravity ($\gamma_1 = \gamma_2 = \gamma$) and the mixed layer depth H_{s0}. For a wide range of parameters, the maximum H_2 ranges from 100 to 200 m. A large reduced gravity obviously prohibits the penetration of the surface Ekman pumping, and therefore inhibits the interior pathway. The mixed layer depth, however, does not have much effect on the interior pathway in the present model. Several ventilated zone

TABLE A1. Maximum H_2 that allows for an interior pathway in the North Pacific.

γ (cm s^{-2})	H_{s0} (m)		
	0	40	80
0.50	195	180	180
1.00	140	125	130
2.00	95	90	100

boundaries for the case of $\gamma = 1$ and $H_{s0} = 0$ have been shown in Fig. 3.

REFERENCES

Fine, R., J. L. Reid, and H. G. Ostlund, 1981: Circulation of tritium in the Pacific Ocean. *J. Phys. Oceanogr.,* **11,** 3–14.

——, W. H. Peterson, and H. G. Ostlund, 1987: The penetration of tritium into the tropical Pacific. *J. Phys. Oceanogr.,* **17,** 553–564.

——, R. Lukas, F. M. Bingham, M. J. Warner, and R. H. Gammon, 1994: The western equatorial Pacific: A water mass crossroads. *J. Geophys. Res.,* **99**(C12), 25 063–25 080.

Godfrey, J. S., 1996: The effect of the Indonesian throughflow on ocean circulation and heat exchange with the atmosphere: A review. *J. Geophys. Res.,* **101**(C5), 12 217–12 237.

——, A. C. Hirst, and J. Wilkin, 1993: Why does the Indonesian throughflow appear to originate from the North Pacific? *J. Phys. Oceanogr.,* **23,** 1087–1098.

Huang, B., 1996: Subtropical–tropical thermocline water exchange in the Pacific. M.S. thesis, University of Wisconsin, 86 pp.

Ji, M., A. Leetmaa, and J. Derbe, 1995: An ocean analysis system for seasonal to interannual climate studies. *Mon. Wea. Rev.,* **123,** 460–481.

Levitus, S., 1982: *Climatological Atlas of the World Ocean.* NOAA Prof. Paper No. 13, U.S. Govt. Printing Office, 173 pp.

Liu, Z., 1994: A simple model of the mass exchange between the subtropical and tropical ocean. *J. Phys. Oceanogr.,* **24,** 1153–1165.

——, S. G. H. Philander, and R. Pacanowski, 1994: A GCM study of tropical–subtropical upper ocean mass exchange. *J. Phys. Oceanogr.,* **24,** 2606–2623.

Lu, P., and J. P. McCreary, 1995: Influence of the ITCZ on the flow of thermocline water from the subtropical to the equatorial Pacific Ocean. *J. Phys. Oceanogr.,* **25,** 3076–3088.

——, ——, and B. Klinger, 1998: Meridional circulation cells and the source waters of the Pacific equatorial undercurrent. *J. Phys. Oceanogr.,* **28,** 62–84.

Lukas, R., T. Yamagata, and J. P. McCreary, 1996: Pacific low-latitude western boundary currents and the Indonesian throughflow. *J. Geophys. Res.,* **101**(C5), 12 209–12 216.

Masumoto, Y., and T. Yamagata, 1991: Response of the western tropical Pacific to the Asian winter monsoon: The generation of the Mindanao Dome. *J. Phys. Oceanogr.,* **21,** 1386–1398.

McCreary, J., and P. Lu, 1994: On the interaction between the subtropical and the equatorial oceans: The subtropical cell. *J. Phys. Oceanogr.,* **24,** 466–497.

McPhaden, M. J., 1996: Monthly period oscillations in the Pacific North Equatorial Countercurrent. *J. Geophys. Res.,* **101,** 6337–6359

——, and R. A. Fine, 1988: A dynamic interpretation of the tritium maximum in the central equatorial Pacific. *J. Phys. Oceanogr.,* **18,** 1454–1457

Talley, L. D., 1985: Ventilation of the subtropical North Pacific: The shallow salinity minimum. *J. Phys. Oceanogr.,* **15,** 633–649.

Tsuchiya, M., R. Lukas, R. Fine, E. Firing, and E. Lindstorm, 1989: Source waters of the Pacific equatorial undercurrent. *Progress in Oceanography,* Vol. 23, Pergamon Press, 101–147.

Wijffles, S., 1993: Exchanges between hemispheres and gyres: A direct approach to the mean circulation of the equatorial Pacific. Ph.D. thesis, MIT/WHOI.

Wyrtki, K., and B. Kilonsky, 1984: Mean water and current structure during the Hawaii-to-Tahiti Shuttle Experiment. *J. Phys. Oceanogr.,* **14,** 242–253.